The Role of Supply Conditions on the Measurement of High-Frequency Emissions

Adam J. Collin, *Member, IEEE*, Antonio Delle Femine, *Member, IEEE*, Carmine Landi, *Senior Member, IEEE*, Roberto Langella, *Senior Member, IEEE*, Mario Luiso, *Member, IEEE*, and Alfredo Testa, *Fellow, IEEE*

***Abstract*— A standardized measurement procedure and source specification for laboratory high-frequency (HF, 2–150 kHz) emissions tests of low-voltage (LV) electronic equipment are still in development. To date, emissions have been measured by direct supply from the mains network or a controllable power source (PS), but both methods are known to interfere with the assessment process. A line impedance stabilization network (LISN) limits supply-load interactions but has been underevaluated until now in the HF analysis, despite being named a potential approach in IEC Standards. This article quantifies the effect of supply conditions on HF emission assessment and the role of the LISN. The effect of the supply voltage fundamental amplitude and low-frequency background distortion on the magnitude and frequency of the characteristic HF emissions is presented, and a new supply configuration combining a programmable PS with LISN is proposed. Experimental results from a case study of two LED lamps with distinct HF emissions, representative of a number of typical LV electronic devices, indicate that only the proposed programmable PS+LISN supply can guarantee the accurate and repeatable measurements under controllable voltage supply conditions and impedance separation that are needed by ongoing HF standardization and modeling activities.**

***Index Terms*— High-frequency (HF) distortion, LED lamps, power quality, power system harmonics, power system measurements.**

I. Introduction

HIGH-FREQUENCY (HF) distortion assessment deals with conducted disturbances in the frequency range from 2 to 150 kHz. The causes and effects of HF distortion have been the subject of research for many years, with a summary and discussion of ongoing areas of research available in [1]. One widely acknowledged open research area is the development of a standardized measurement method that assures accurate and repeatable emission measurements of low-voltage (LV) equipment. Currently, HF distortion assessment procedures are covered by the Informative Annexes of IEC Standards 61000-4-7 [2] and 61000-4-30 [3]. These methods have been proposed from the perspective of *in situ*, i.e., long-term, power quality monitoring, with a particular emphasis given to voltage distortion compliance assessment. As such, there is little guidance on the supply system configuration for laboratory measurements of HF emissions.

Two supply configurations have been predominantly used in literature: supply from the mains network, e.g., [4]–[6], or from a programmable power source (PS) for laboratory experiments, e.g., [7]–[10]. With both configurations, it is possible for the source to exert influence on the equipment under test (EUT): from the mains network, due to the existing HF voltage distortion and possible impedance resonance conditions, or from a PS, whose spurious HF content has been identified as a cause of measurement uncertainty [7]. Without a clear understanding and control of the complex interactions between the EUT and the impedance and background voltage distortion of the supply, it is impossible to properly identify the "characteristic" HF emissions of the EUT, i.e., the emissions present when the EUT is supplied with an ideal sinusoidal voltage of rated magnitude and frequency (analogous to the classical definition of characteristic harmonics in [11]).

Defining a repeatable measurement procedure for identifying the characteristic HF emissions is a crucial step toward understanding the long-term implications of HF distortion. To this end, the CISPR 16-1-2 method [12] has been suggested in IEC Std 61000-4-7 [2] and 61000-4-30 [3]. This method incorporates a line impedance stabilization network (LISN) aimed at decoupling the EUT from HF interference from the supply. Despite this benefit, the LISN has not been widely utilized by the power systems scientific community to measure HF emissions, with recent attention only in [13] and [14], where the LISN is utilized without considering its ability to separate the voltage between the supply and the EUT at HF.

Reference [14] provided an initial assessment of HF emissions by comparing the results of only three different supply configurations of the measurement setup: mains, mains with LISN, and PS without LISN. This study highlighted and quantified the impact on the HF emission measurement results of the HF background distortion and the HF coupling

Manuscript received December 6, 2019; revised February 18, 2020; accepted April 7, 2020. Date of publication May 18, 2020; date of current version August 11, 2020. This work was supported in part by the Italian Ministry of University and Research under Grant PON03PE-00178-1, in part by the University of Campania "Luigi Vanvitelli" through the funding program V:ALERE 2019 under SEEM Grant, and in part by the European Metrology Program of the Innovation and Research (EMPIR) 18NRM05 SupraEMI Project (EMPIR is jointly funded by the EMPIR participating countries within EURAMET and the European Union). The Associate Editor coordinating the review process was Ferdinanda Ponci. *(Corresponding author: Adam J. Collin.)*

The authors are with the Department of Engineering, University of Campania "Luigi Vanvitelli," 81031 Aversa, Italy (e-mail: adam.collin@ieee.org).

Color versions of one or more of the figures in this article are available online at http://ieeexplore.ieee.org.

Digital Object Identifier 10.1109/TIM.2020.2992824

impedance of the supply configuration. However, the effect of the fundamental amplitude and low-frequency (LF) background distortion of supply voltages on the EUT HF emissions was not considered.

This article completes the work in [14] by introducing the effects of the supply voltage fundamental amplitude and LF background distortion on the HF emissions of the EUT and proposes a new supply configuration combining a programmable PS with LISN suitable for this analysis. An analytical and experimental evaluation of the LISN is also provided, with particular emphasis given to its supply-load voltage decoupling feature over the entire HF range.

Further metrological extensions from [14] are as follows: all components of the measurement chain have been characterized in the HF range, and a more thorough measurement campaign of the supply voltage LF and HF background distortion has been performed. The experimental results, from two LED lamps with distinctive HF emissions, have also been extended and clearly demonstrate the impact of variations of the voltage fundamental and LF distortion on the HF emission assessment of power electronic devices. These results evidence the need to combine a programmable PS and LISN for accurate and repeatable measurements under fully controllable supply conditions, both at fundamental and LFs, and with HF voltage and impedance separation. The newly proposed supply configuration can be used to develop models of HF emissions and provides a stable means to evaluate HF distortion assessment techniques.

The rest of this article is structured as follows. The measurement setups are described in Section II. Section III provides a technical appraisal of the LISN. The LF and HF distortions of the supply voltage are discussed in Section IV. Section V presents a study on the identification of the HF emissions of LED lamps. Conclusions are offered in Section VI.

II. Measurement Setups

A. Descriptions

A new measurement setup, consisting of a programmable PS plus LISN, is proposed in this article and shown in Fig. 1(d), in addition to the three setups discussed in [14]. Each consists of a supply configuration and the same measurement chain.

The defining features of the measurement setups are the source, either mains or programmable PS, and the presence, or not, of the LISN. As such, these are referred to as mains [see Fig. 1(a)], mains+LISN [see Fig. 1(b)], PS [see Fig. 1(c)], and PS+LISN [see Fig. 1(d)] from hereon. Due to the high earth leakage current of the LISN, an isolating transformer (IT) was inserted between the source and the LISN to avoid tripping the differential protection. As they operate together, the combination is referred to as LISN, unless a distinction between the IT and LISN is pertinent to the discussion.

The measurement chain was constituted by a current transducer (CT), a voltage transducer (VT), and a data acquisition (DAQ) system. The CT utilized was the Pearson Current Monitor Model 411 (50 A/5 V, 1%, 1 Hz–20 MHz), and the VT used was the LEM CV3-1000 (700 V/7 V, 0.2 %, 0–500 kHz). The National Instruments (NI) PCI eXtension for Instrumentation (PXI) 5922 board (24 bit, 5 V, 500 kHz), housed in a PXI chassis running the measurement software (developed in LabVIEW), was used as the DAQ. The programmable PS was the Pacific Power 3120 AMX (3-phase, 12 kVA, 20 Hz–5 kHz).

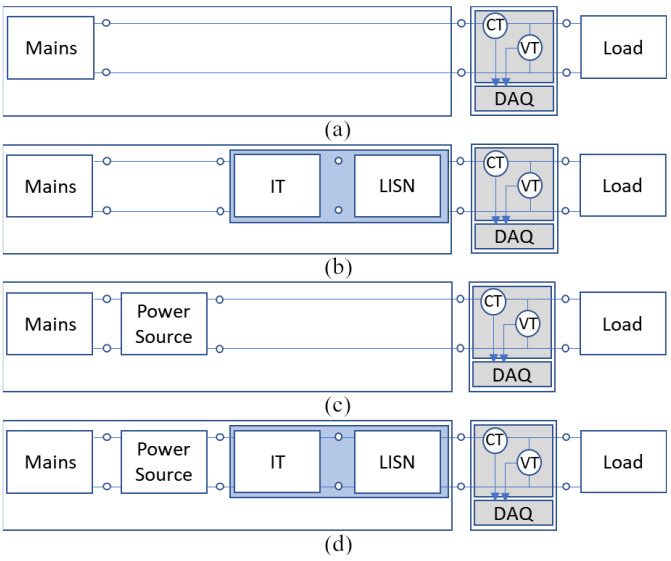

Fig. 1. Measurement setup configurations. (a) Mains supply. (b) Mains+LISN supply. (c) PS supply. (d) PS+LISN supply.

B. Measurement Chain Characterization

In order to assess and compensate for any systematic errors, the elements of the measurement chain have been characterized.

1) DAQ: The gain of the two input channels of the DAQ-PXI was measured. The multifunction calibrator Fluke 5730A was used as the reference instrument for this test. Sinusoidal voltages, with fixed root-mean-square (rms) amplitude of 1.75 V (i.e., about half of the input full-scale range) and frequency stepped from 50 Hz to 150 kHz, were generated and simultaneously acquired by the two channels at a sampling rate of 500 kHz (the same used for all experimental tests). Results are not shown for sake of brevity; however, the maximum ratio error ϵ_r was 240 μV/V with expanded uncertainty U_c (99% confidence level, the definition used from hereon) of 600 μV/V (due to the Type-B uncertainty of the calibrator).

2) Voltage Transducer: The VT was characterized using the Fluke 5730A as a voltage source, with two Fluke 8508A Digital MultiMeters (DMMs) used to measure the input and the output of the VT. In the first step, the two DMMs (one set to the 200-V input range and one set to the 2-V range) were supplied with the same sine waves, with a fixed amplitude of 1.95 V_{rms} and frequency stepped from 50 Hz to 150 kHz. This measured the mismatch of their magnitude frequency responses and was treated as a systematic error. In the second step, sine waves, with a fixed amplitude of 100 V_{rms} and frequency stepped from 50 Hz to 150 kHz, were supplied to the VT. The measured VT ϵ_r was compensated using the

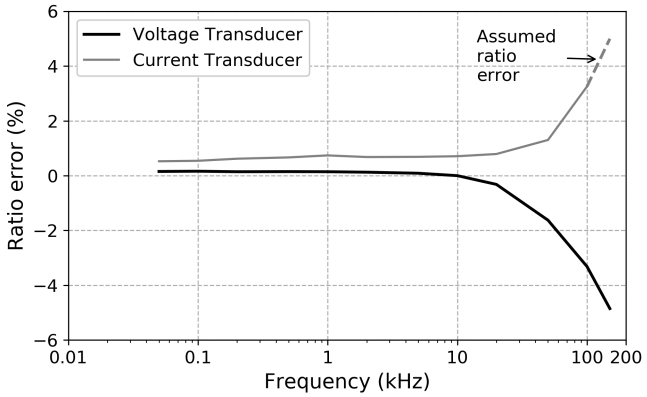

Fig. 2. Ratio errors of the VT (black) and CT (gray) from 50 Hz up to 150 and 100 kHz, respectively.

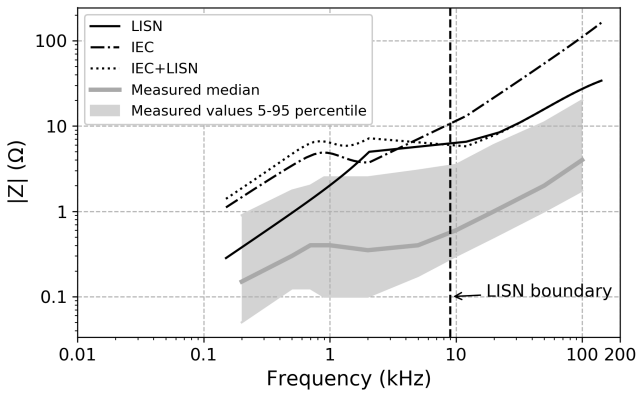

Fig. 3. Comparison of LISN impedance values with the AMN from IEC Std 61000-4-7 [2] and measured LV networks [17].

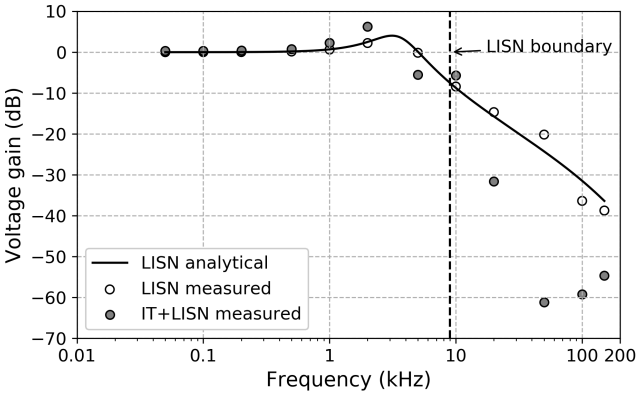

Fig. 4. Voltage gain from supply to load of the ideal LISN (solid line) and the measured gain of the LISN (white symbols) and the combined IT+LISN (gray symbols).

DMMs systematic error. The maximum U_c (at 150 kHz) of the VT ϵ_r is 500 μV/V. The VT ϵ_r is shown in Fig. 2.

3) Current Transducer: The CT was characterized using the reference shunt Fluke A40B 1/0.8 A/V (100 kHz, 30 μV/V). The current signal was obtained from the transconductance amplifier Fluke 52120A driven by the calibrator Fluke 5730A. Sine waves with an amplitude of 1 A_{rms} and frequency from 50 Hz to 100 kHz were supplied to the two transducers; their outputs were simultaneously acquired with the two channels of the DAQ at 500 kHz, and the rms values of the signals were evaluated. The CT has been characterized up to 100 kHz as this is the certified range of the reference shunt. The measured CT ϵ_r was compensated using the DAQ systematic error. The maximum U_c (at 100 kHz) of the CT ϵ_r is 400 μV/V. Above 100 kHz, ϵ_r has been obtained by linear interpolation. The CT ϵ_r is shown in Fig. 2.

The measured ϵ_r values have been used to compensate the magnitudes of the measured spectral components by performing multiplication in the frequency domain. The final expanded uncertainties on all measured spectral components, after compensating the systematic ϵ_r of the DAQ, VT, and CT, are 980 μV/V at 150 kHz and 940 μA/A at 100 kHz. These values include the contribution of the desynchronized processing technique (DPT) [15] used during the analysis, quantified as 200 μV/V or μA/A (standard uncertainty).

III. Technical Appraisal of the LISN

Despite inclusion in [2], the LISN has not been widely utilized in HF measurements in power systems and should be assessed in this context. The features of the LISN are as follows.

1) It offers a defined and stable impedance and is theoretically unaffected by the impedance of the supply.
2) It acts as a low-pass filter of the supply voltage.
3) It provides a means to obtain repeatable measurements.

The LISN also couples the HF emissions of the EUT into a coaxial radio frequency (RF) receiver. Although the RF output of the LISN utilizes more of the DAQ input range for the HF emission measurement (i.e., measuring with higher accuracy), the current signals were obtained using the CT. In this way, all configurations were affected by the same uncertainty and can be directly compared. In this mode, the LISN RF output is terminated by a 50-Ω impedance [16].

When utilized to measure HF emissions in power systems, in which considerable background voltage distortion may be present, the voltage gain of the LISN plays a significant role. However, this is not widely reported in the literature.

A. Stabilization of Supply-Side Impedance

One of the key functions of the LISN is to provide a stable impedance to the EUT. The short-circuit impedance of the reference LISN, as shown in Fig. 3, is widely reported in literature. However, to justify its use for assessing HF emissions in power systems, the LISN impedance values must be compared with network impedances. For this reason, the impedance of the artificial mains network (AMN) from IEC Std 61000-4-7 [2], in isolation and in cascade with the LISN, and impedance values measured in LV networks in Europe ([17]) are also shown. From Fig. 3, it is possible to deduce that although the LISN impedance may be higher than values from [17], the trend with respect to frequency is preserved.

B. Attenuation of Supply-Side HF Voltage Distortion

The magnitude frequency response of the device composed of the cascade connection of the IT+LISN has been characterized by the PS (used as an amplifier and driven by the Arbitrary Waveform Generator NI 5422 housed in the PXI chassis).

Waveforms composed by a fundamental component, 230 Vrms at 50 Hz, and a harmonic tone, with a fixed amplitude of 10% of the fundamental tone, zero phase, and frequency stepped from 100 Hz to 150 kHz, were used. The input and the output of the combined IT+LISN were measured through two VTs and two channels of the DAQ. Through the measurement of their rms values, the magnitude frequency response has been evaluated and compensated using the systematic ϵ_r between the two VTs and the two DAQ channels. The measured magnitude frequency response is shown in Fig. 4, alongside the voltage gain obtained from an analytical model of the ideal LISN. Good matching between the analytical model and measurements without the IT is evident. The presence of the IT increases the attenuation at frequencies over 20 kHz.

IV. Background Voltage Distortion

The characteristics of the background voltage will inherently influence the outcome of any HF emission assessment. HF components present in the background voltage may be absorbed by the EUT and erroneously considered an HF current injection from the EUT if the presence of the component is not known *a priori*. The LF characteristics should also be assessed to quantify their impact on HF emissions.

To assess the background voltage distortion of the measurement setups, no-load tests were performed throughout the test period. The waveforms were processed using the method in [14], utilizing a DPT to reduce the effect of harmonic spectral leakage [15]. No further processing was performed on the LF components; the HF components were grouped using the method in [2]. The measurements were performed across multiple days to capture variations in the supply conditions; in total, 1330 individual 200-ms windows were recorded over four days. Results of the mean and 5%–95% boundary values for LF components are in Fig. 5 and the HF distortion in Fig. 6.

A. Low Frequency

The results in Fig. 5 clearly show that the (expected) LF components present in the mains supply are not attenuated by the LISN but are amplified, in accordance with results in Fig. 4. However, the presence of the LISN has only a minor (negative) impact on LF frequency components as demonstrated by the total harmonic distortion (THD) mean (and standard deviation) values that increase from 2.24 (0.1)% to 2.37 (0.11)%. This effect is also observed in the PS+LISN supply configuration, but, here, the magnitudes are much lower, with THD increasing from 0.02 (0.0006)% to 0.21 (0.006)%.

In Fig. 5, a zoomed-in view of the fundamental frequency is also shown. The systematic increase of the mains+LISN measurement setup voltage is a consequence of the loading condition of the IT and is very difficult to compensate during real-time measurements. However, this is possible when using PS+LISN, by applying a waveform with lower amplitude at the input of the PS amplifier (which has fixed voltage gain).

B. High Frequency

In Fig. 6, it is evident that the mains supply is characterized by several prominent tones with the highest magnitude

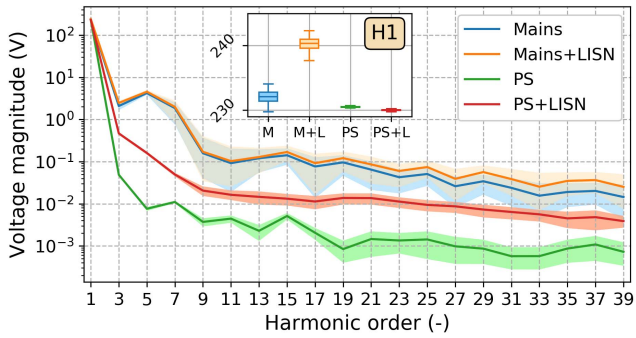

Fig. 5. Mean value and 5%–95% range (shown as shaded areas) of the LF background voltages recorded during the test period.

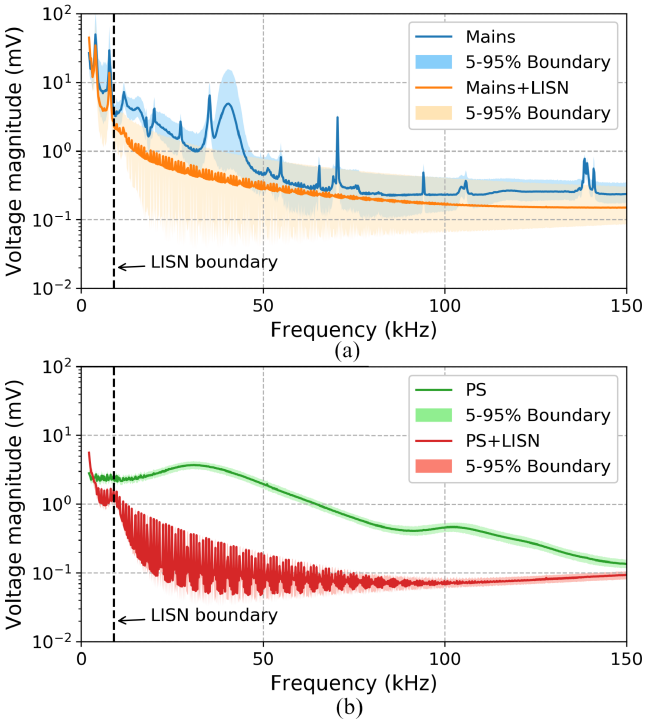

Fig. 6. Mean value and 5%–95% range of HF background voltage distortion recorded during the test period of (a) mains and mains+LISN and (b) PS and PS+LISN.

observed of any measurement chain, ranging from 0.3 to 100 mV. However, in the frequency range 10–50 kHz, the magnitude of the background voltage distortion of the PS is 2-5 mV. The THD in the HF range is around 0.1%, lower than the manufacturers' guarantee (THD $<$ 0.25% up to 5 kHz).

When the mains or PS supply are combined with the LISN, two effects are observed. Above the minimum design frequency of the LISN (i.e., 9 kHz), the background voltage distortion of both supplies is considerably attenuated. When operating with the mains supply, the 2–9-kHz components may not be significantly suppressed, in accordance with Fig. 4. However, the combined effect of the PS+LISN supply has a twofold benefit: the LISN attenuates the HF components of the PS, while the distortion produced by the PS in the range 2–9 kHz is considerably lower than that present in the mains. Although the supply impedance can also influence the outcome of the HF assessment, based on these results, it is evident that

the background voltage distortion of the mains and PS supply configurations will have the dominant effect.

C. Discussion

It is possible to conclude the following.

1) Mains supply is not stable and includes LF and HF tones.
2) Mains+LISN is better as there is the attenuation of the HF voltage distortion, but fundamental and LF distortion are not controllable and long term measurements are needed to extract the mean values.
3) PS is stable but presents a consistently high-value background distortion in the HF range.
4) PS+LISN is stable and combines the control of the LF components with low values of HF voltage distortion.

V. Case Study: Characteristic High-Frequency Emissions of LED Lamps

LED lamps have been selected for the experimental analysis. From the different topologies of LED drivers, two (defined as Type A and Type D, of 12 and 40 W, respectively) have been selected. The circuit topologies and control algorithms of the selected LED lamps are representative of several different LV electronic devices, including the majority of power electronic loads and electric vehicle chargers.

Type A LED lamps contain an offline switch-mode driver circuit (SMDC) constituted by a full-wave rectifier with a smoothing capacitor that feeds a dc–dc converter to regulate the output to the LED chain. Type D LED lamps are equipped with single- or double-stage SMDC with active or passive power factor correction units with input current closed- or open-loop control circuits. Further details are available in [18].

A. Test Procedure

The test procedure defined in [14] has been utilized for the HF distortion assessment. In this procedure, digital filtering is achieved by means of a DPT [15], to minimize the effect of spectral leakage, and the IEC Std 61000-4-7 test protocol has been implemented for spectral analysis of the components, resulting in a frequency resolution of 200 Hz [2].

Each test consisted of a sequential application of each measurement setup to ensure that inherent short-term variations in the mains supply are also captured by the mains+LISN supply. The delay between the measurements of different measurement setups was approximately 10 s, including the time required to measure and process the signal and write the data file. Each test recorded 2 s of data, i.e., 10×200 ms analysis windows, with a 500-kHz sample rate. Tests were repeated at regularly spaced intervals, selected as 5 min in this article, during that time the EUT and the measurement setup components were maintained in an active state.

B. Measurement Condition Stability

Consideration of the measurement condition is crucial to provide a fair comparison between the measurement setups.

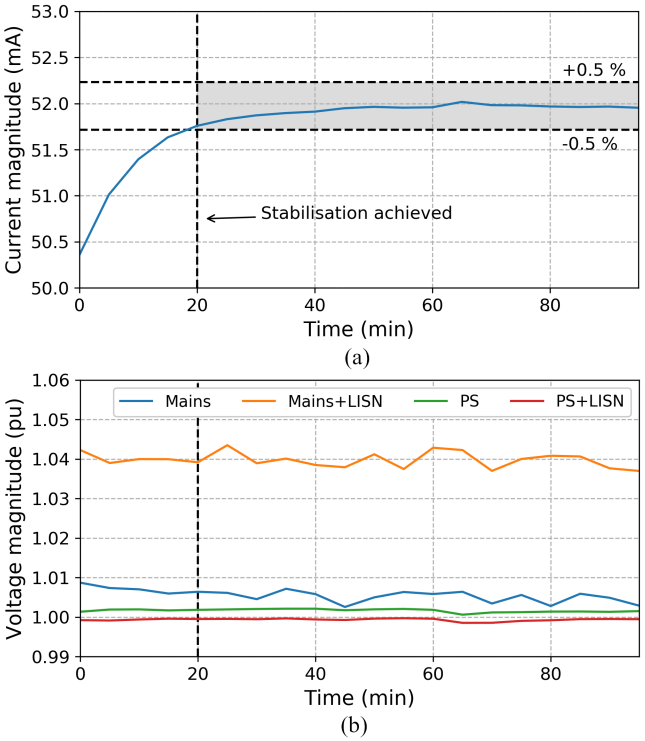

Fig. 7. Fundamental current and voltage rms values measured during a test period of the Type A LED lamp. (a) Current. (b) Voltage. Stabilization is marked by the horizontal line.

The light output of LEDs, and hence the absorbed current, requires a period of time to stabilize, with values up to 1 h reported in [19]. In the presented analysis, the fundamental current is considered as the indicator, with a value of ±0.5% of the steady-state value taken as acceptable. Accordingly, values considered for analysis were those measured after this threshold had been reached. The threshold choice is arbitrary but considered acceptable for comparing the measurement setups. The variation in the Type A LED lamp fundamental current during an exemplar test is presented in Fig. 7(a), where the ±0.5% threshold is obtained after 20 min.

The corresponding fundamental voltage values are presented in Fig. 7(b). For the considered test, there is a small decrease in the mains supply voltage but less than 1% of the rated value. The systematic increase in the mains+LISN measurement setup voltage has already been discussed in Section IV-A. The results in Fig. 7(b) confirm good regulation of the supply voltage magnitude in the PS and PS+LISN measurements setups, which are within ±0.25% of the rated voltage.

C. Type A LED Lamp

HF current emission values are shown in Fig. 8. In the values measured with the mains supply, it is impossible to discern the characteristic emissions of the EUT from the background distortion (see Fig. 6). The largest components in the current are found at 40 and 75 kHz and display different responses. The magnitude of the tone at 40 kHz is highly variable, while the magnitude of the tone at 70 kHz is constant. Without the extensive background voltage measurement

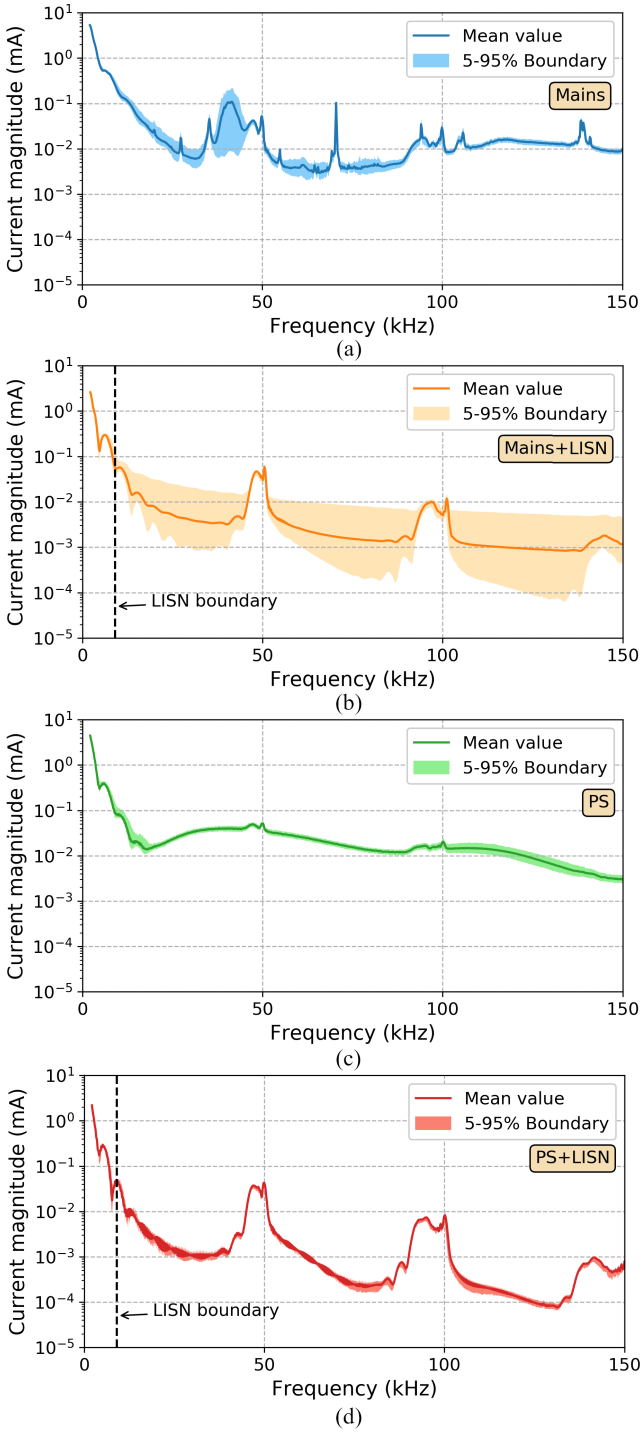

Fig. 8. HF current emission values of the Type A LED lamp measured with (a) mains supply, (b) Mains+LISN supply, (c) PS supply, and (d) PS+LISN supply.

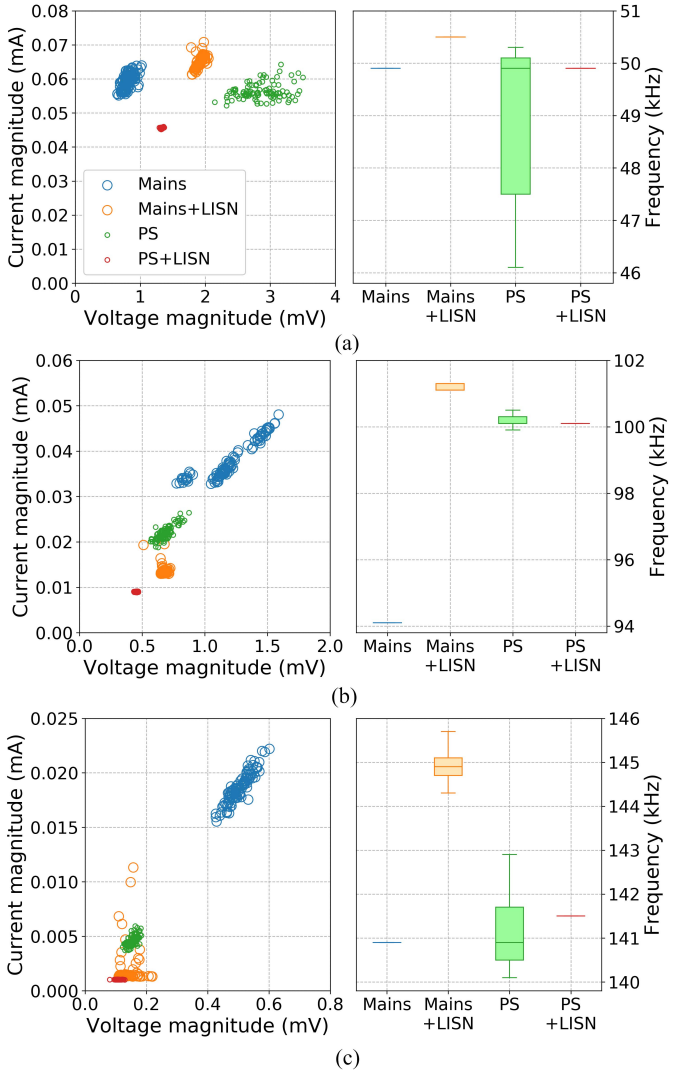

Fig. 9. Magnitude and frequency analysis of the three current emission frequency ranges identified from the measurement of the Type A LED lamp. (a) Range I. (b) Range II. (c) Range III.

campaign presented in Section IV, i.e., *a priori* knowledge, these components could be mistakenly considered as HF emissions from the EUT, rather than current absorbed by the load impedance. When combining the mains+LISN, the characteristic emissions are visible, but there is a large instability, up to two orders of magnitude, due to the absorption of the background voltage distortion.

With only the programmable PS, the HF tones are not discernible from the background, as observed in [7]. Although the components around 50 and 100 kHz are observed in a visual inspection, their magnitude is comparable to the background (a difference well below 3 dB) and, thus, cannot be assessed with confidence.

Combining the PS+LISN, three distinct, and stable, frequency ranges (families) of current injections are clearly visible at Range I: 46–50.5 kHz, Range II: 94–101 kHz, and Range III: 140–146 kHz. The ranges appear to correspond to integer multiples of the switching frequency of the dc-dc converter present in the lamp, with wideband emission due to its specific control algorithm.

A more detailed representation of the magnitude variation of the current versus the voltage and the frequency distribution of the maximum current frequency bin extracted from measurements in the three frequency ranges is shown in Fig. 9.

For the first frequency range, there is no obvious correlation between the groups of points. As such, the dispersion can be assumed to be due to inherent variations in the operation of both the EUT and the individual components that constitute each measurement setup. In this range, the mean value of the

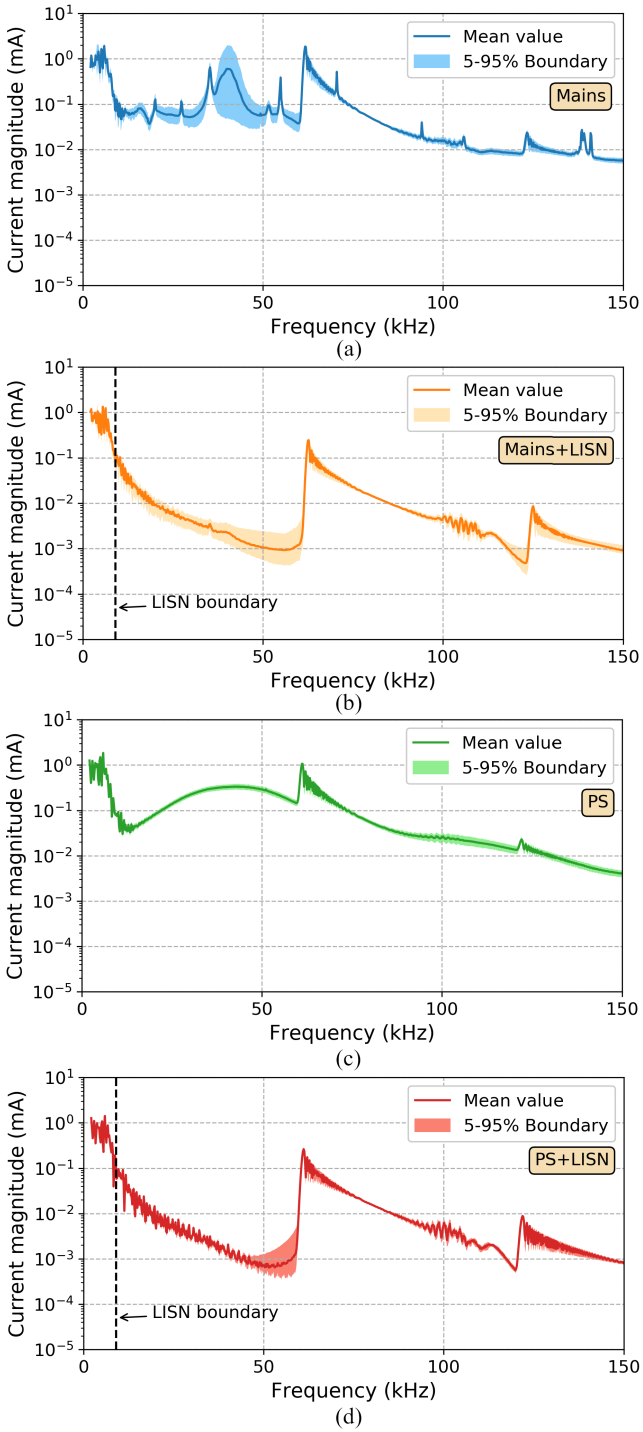

Fig. 10. HF current emission values of the Type D LED lamp measured with (a) mains supply, (b) Mains+LISN supply, (c) PS supply, and (d) PS+LISN supply.

maximum frequency is the same for the mains, the PS and PS+LISN supply, with a range of variation for the PS case of almost 5 kHz. The higher frequency of the mains+LISN result is a result of the higher magnitude of the supply voltage and is observed in all three frequency ranges, i.e., it is systematic.

In the second frequency range, the mains supply presents a false positive for the frequency value. It appears stable but corresponds to a component present in the background. This occurs in the third frequency range for both mains and PS

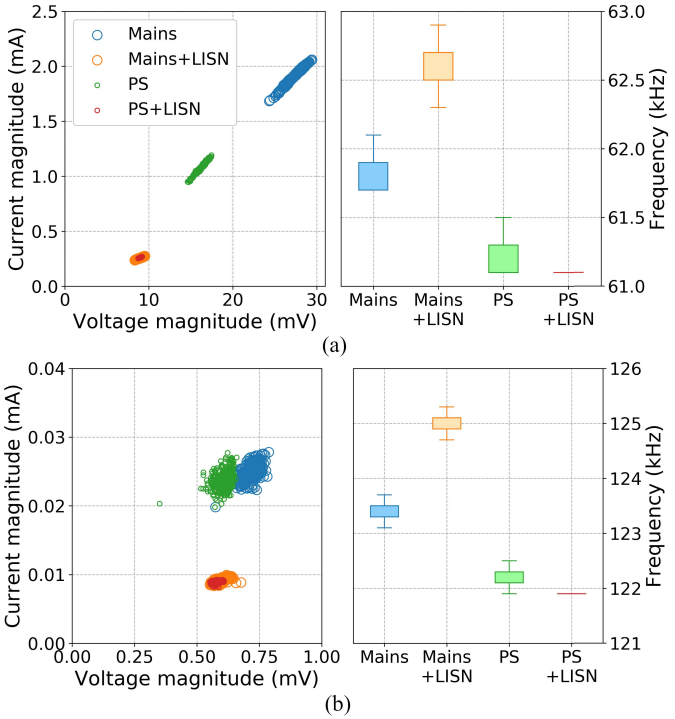

Fig. 11. Magnitude and frequency analysis of the two current emission frequency ranges identified from the measurement of the Type D LED lamp. (a) Range I. (b) Range II.

supplies. In this way, the ratio between the current and voltage magnitude appears as an impedance-like relationship; however, due to the complex nature of interactions in the HF range, and also the impact of LF phenomena, it is difficult to draw firm conclusions on the exact frequency response.

In all cases, the stability of the values obtained using the PS+LISN supply is clearly visible.

D. Type D LED Lamp

HF current emission values are shown in Fig. 10. The broad conclusions are similar to the Type A LED lamp; however, the stability of the mains+LISN measurement during the test period is improved for this type of LED lamp, and the peak is (just) visible around 125 kHz using the PS supply. Generally, the HF tones are more pronounced with respect to the Type A LED lamp due to the higher rated power of this LED lamp.

Combining PS+LISN, two distinct, and stable, frequency ranges (families) of current injections are clearly visible at Range I: 60–64 kHz and Range II: 120–126 kHz. Again, the ranges appear to correspond to integer multiples of the switching frequency of the dc-dc converter present in the lamp. Assessment of the peak current values, after 9 kHz, is shown in Fig. 11.

There are marked differences in the assessment of the first peak. Compared with the values measured with the LISN, the current values are $\times 4$ and $\times 8$, respectively, when using the PS and mains in isolation, with voltage $\times 2$ and $\times 4$. The linear ratio observed between the voltage and current indicates an impedance behavior. In the second frequency range, a constant

current source is identified for the peak value with the LISN. There is higher variability with mains and PS, but there appears to be a fixed ratio, suggesting that the difference in results is due to the higher impedance of the LISN.

For this test, no false positives are returned by any measurement chain. As such, it is possible to directly compare the values obtained. From these results, it is possible to observe that the characteristic HF emission of this equipment is sensitive to both the magnitude and the shape, i.e., LF harmonics, of the supply voltage waveform. This is evident as the frequency observed with mains supply, i.e., with different waveform shapes, is higher in both frequency ranges than the (approximately) ideal sinusoidal waveform of the PS and PS+LISN supplies. Furthermore, the frequency observed with the mains+LISN supply is again higher than the mains supply, as both waveforms have the same LF harmonics, suggesting sensitivity to the supply voltage magnitude.

E. Effects of Supply Voltage Fundamental Amplitude and Waveform Shape

The effect of the supply voltage fundamental amplitude and the waveform shape on the LF emissions of LED lamps is widely reported, e.g., [7], [20]; however, their effect on the characteristic HF emissions of lamps has not yet been widely reported in literature. The results in Sections V-C and V-D indicate that some of the differences in values of HF emissions reported may be due to the fundamental amplitude and waveform shape, which is different for mains and PS (with or without LISN). To confirm this hypothesis, some experiments, designed to analyze the effects of supply voltage fundamental amplitude and shape, have been performed using the only supply configuration, which allows this kind of experiment: PS+LISN.

Fig. 12 shows the sensitivity of the HF current emissions in frequency Range I to variations of supply voltage in terms of fundamental amplitude (from 0.9 to 1.1 p.u.) and waveform shape for the Type A and Type D LED lamps. The waveform shapes considered are an ideal sinusoid (SIN) and standardized distorted shapes typical of residential, flat top (FT), and industrial, peak top (PK), distribution systems [21]. It is possible to observe the following.

1) For a fixed fundamental amplitude, the frequency variation reaches plus 3% for the Type A LED lamp and 6% for the Type D LED lamp, from the minimum (at 0.9 p.u.) to the maximum observed values, for all shapes and amplitudes, and the amplitude variation reaches plus 100% from the minimum to the maximum observed values for the Type A LED lamp and plus 15% for the Type D LED lamp, both in the case of fundamental amplitude equal to 0.9 p.u.
2) For a fixed shape, the frequency variation is around 10% from the minimum to the maximum observed values for both types of LED lamp and all shapes, and the amplitude variation reaches almost plus 50%, from the minimum to the maximum observed values, for the Type A LED lamp in the case of FT and plus 100% for the Type D LED lamp for all voltage waveforms.

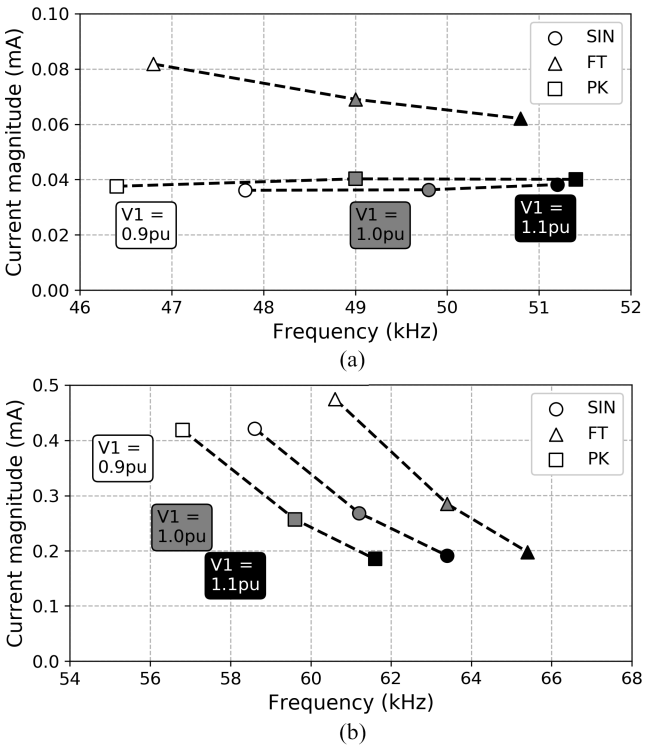

Fig. 12. Sensitivity of the Range I HF current emissions to variations in supply voltage fundamental amplitude (V1 = 0.9–1.1 p.u.) and shape (sinusoidal-SIN, flat top-FT, and peak top-PK) of (a) Type A LED lamp and (b) Type D LED lamp.

F. Final Discussion

The results reported earlier highlight the dominant role played by LF background distortion present in the supply configuration during measurements to characterize the HF emissions of LED lamps. The differences between the analyzed supply configurations are also evidenced in Figs. 5 and 7(b). In general, the relevant literature demonstrates the importance of characterizing power electronic equipment under different reference supply conditions both for modeling and emission assessment purposes [7], [20].

The abovementioned considerations confirm the conclusion that the only measurement setup for laboratory experiments able to perform a comprehensive and repeatable HF distortion analysis is that proposed in this article: a supply configuration constituted by a fully programmable PS to control supply voltage at fundamental and LF together with an LISN to ensure impedance stability at HF.

VI. Conclusion

A standardized measurement procedure and source specification for laboratory HF (2–150 kHz) emissions tests of LV electronic equipment are still in development. The most common approaches to assess HF emissions have been to use direct supply from the mains network or a controllable PS, but both sources can interfere with the assessment process. LISNs limit supply-load interactions, but this component has been underevaluated in the HF analysis up until now, despite being named a potential approach in IEC Standards.

This article has completed previous research by the same authors on the effect of supply conditions on HF emission assessment and the role of the LISN. The effect of the supply voltage fundamental amplitude and LF background distortion on the magnitude and frequency of the characteristic HF emissions has been presented, and a new supply configuration, combining a programmable PS with an LISN, has been proposed.

All components of the measurement chain have been characterized, and it was shown that the accuracy of the measurement chain components, i.e., the DAQ, CT, and VT, could be lower than those declared by the manufacturers and also frequency dependent. Therefore, the measurement chain should be properly characterized, and the systematic errors compensated, to avoid introducing inaccuracies into the analysis.

The experimental case study results, constituted by two LED lamps with distinct HF emissions, representative of a number of typical LV electronic equipment, have indicated that the only measurement setup for laboratory experiments able to perform a comprehensive and repeatable HF distortion analysis is that proposed in this article: a supply configuration constituted by a fully programmable PS, to control supply voltage at fundamental and LFs, together with an LISN, to ensure impedance stability at HF.

ACKNOWLEDGMENT

This article was prepared at the SUN-EMC Laboratory, University of Campania "Luigi Vanvitelli."

REFERENCES

[1] S. K. Ronnberg *et al.*, "On waveform distortion in the frequency range of 2 kHz–150 kHz—Review and research challenges," *Electr. Power Syst. Res.*, vol. 150, pp. 1–10, Sep. 2017.

[2] *Testing and Measurement Techniques—General Guide on Harmonics and Interharmonics Measurements and Instrumentation, for Power Supply Systems and Equipment Connected Thereto*, Standard IEC 61000-4-7, 2002.

[3] *Testing and Measurement Techniques—Power Quality Measurement Methods*, IEC Standard 61000-4-30, 2015.

[4] S. K. Ronnberg, M. Wahlberg, M. H. J. Bollen, and C. M. Lundmark, "Equipment currents in the frequency range 9–95 kHz, measured in a realistic environment," in *Proc. 13th Int. Conf. Harmon. Qual. Power*, Wollongong, NSW, Australia, Sep. 2008, pp. 1–8.

[5] E. O. A. Larsson, M. H. J. Bollen, M. G. Wahlberg, C. M. Lundmark, and S. K. Ronnberg, "Measurements of high-frequency (2–150 kHz) distortion in low-voltage networks," *IEEE Trans. Power Del.*, vol. 25, no. 3, pp. 1749–1757, Jul. 2010.

[6] A. Larsson and M. Bollen, "Emission (2 to 150 kHz) from a light installation," in *Proc. 21st Int. Conf Electr. Distrib. (CIRED)*, Jun. 2011, pp. 1–4.

[7] A. Gil-De-Castro, R. Medina-Gracia, S. K. Ronnberg, A. M. Blanco, and J. Meyer, "Differences in the performance between CFL and LED lamps under different voltage distortions," in *Proc. 18th Int. Conf. Harmon. Qual. Power (ICHQP)*, Ljubljana, Slovenia, May 2018, pp. 1–6.

[8] A. Grevener, J. Meyer, S. Rönnberg, M. Bollen, and J. Myrzik, "Survey of supraharmonic emission of household appliances," *CIRED-Open Access Proc. J.*, vol. 2017, no. 1, pp. 870–874, Oct. 2017.

[9] S. Schottke, J. Meyer, P. Schegner, and S. Bachmann, "Emission in the frequency range of 2 kHz to 150 kHz caused by electrical vehicle charging," in *Proc. Int. Symp. Electromagn. Compat.*, Gothenburg, Sweden, Sep. 2014, pp. 620–625.

[10] D. Darmawardana, S. Perera, J. Meyer, D. Robinson, U. Jayatunga, and S. Elphick, "Development of high frequency (supraharmonic) models of smallscale (<5 kW), single-phase, grid-tied PV inverters based on laboratory experiments," *Electr. Power Syst. Res.*, vol. 177, Dec. 2019, Art. no. 105990.

[11] J. Arrillaga and N R. Watson, *Power System Harmonics*, 2nd ed. New York, NY, USA: Wiley, 2003.

[12] *Specification for Radio Disturbance and Immunity Measuring Apparatus and Methods—Part 1-2: Radio Disturbance and Immunity Measuring Apparatus-Coupling Devices for Conducted Disturbance Measurements*, Standard CISPR 16-1-2:2014+A1:2017, 2017.

[13] D. Agudelo-Martinez, A. Pavas, A. M. Blanco, R. Stiegler, and J. Meyer, "Influence of measurement setup on the emission of devices in the frequency range 2-150 KHz," in *Proc. IEEE Milan PowerTech*, Milan, Italy, Jun. 2019, pp. 1–6.

[14] A. J. Collin, A. D. Femine, C. Landi, R. Langella, M. Luiso, and A. Testa, "Assessment of the high frequency emissions of low-voltage electronic equipment under different supply conditions," in *Proc. IEEE 10th Int. Workshop Appl. Meas. Power Syst. (AMPS)*, Aachen, Germany, Sep. 2019, pp. 1–6.

[15] A. J. Collin, S. Z. Djokic, J. Drapela, R. Langella, and A. Testa, "Proposal of a desynchronized processing technique for assessing high-frequency distortion in power systems," *IEEE Trans. Instrum. Meas.*, vol. 68, no. 10, pp. 3883–3891, Oct. 2019.

[16] *American National Standard for Methods of Measurement of Radio Noise Emissions from Low-Voltage Electrical and Electronic Equipment in the Range of 9 kHz to 40 GHz*, Standard ANSI C63, Jun. 2014.

[17] R. Stiegler *et al.*, "Survey of network impedance in the frequency range 2-9 kHz in public low voltage networks in AT/CH/CZ/GE," in *Proc. 25th Int. Conf. Electr. Distrib.*, 2019, pp. 1–5.

[18] A. J. Collin, S. Z. Djokic, J. Drapela, R. Langella, and A. Testa, "Light flicker and power factor labels for comparing LED lamp performance," *IEEE Trans. Ind. Appl.*, vol. 55, no. 6, pp. 7062–7070, Nov./Dec. 2019.

[19] S. Sakar, S. Ronnberg, and M. H. J. Bollen, "Light intensity behavior of LED lamps within the thermal stabilization period," in *Proc. 18th Int. Conf. Harmon. Qual. Power (ICHQP)*, Ljubljana, Slovenia, May 2018, pp. 1–6.

[20] X. Xu, A. Collin, S. Z. Djokic, R. Langella, A. Testa, and J. Drapela, "Experimental evaluation and classification of LED lamps for typical residential applications," in *Proc. IEEE PES Innov. Smart Grid Technol. Conf. Eur. (ISGT-Europe)*, Turin, Italy, Sep. 2017, pp. 1–6.

[21] *Testing and Measurement Techniques Harmonics and Interharmonics Including Mains Signalling at A.C. Power Port, Low Frequency Immunity Tests*, Standard IEC 61000-4-13, 2015.

Adam J. Collin (Member, IEEE) was born in Edinburgh, U.K., in April 1985. He received the B.Eng. degree in electrical and electronic engineering from The University of Edinburgh, Edinburgh, in 2007, the M.Sc. degree in renewable energy and distributed generation from Heriot-Watt University, Edinburgh, in 2008, and the Ph.D. degree from The University of Edinburgh in 2013.

He is currently a Researcher with the University of Campania "Luigi Vanvitelli," Aversa, Italy. His research interests include power system harmonics, load modeling, and distribution system analysis.

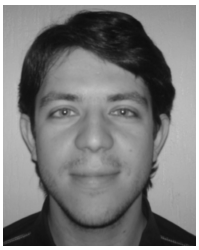

Antonio Delle Femine (Member, IEEE) was born in Caserta, Italy, in March 1980. He received the M.Sc. degree *(summa cum laude)* in electronic engineering and the Ph.D. degree in electrical energy conversion from the University of Campania "Luigi Vanvitelli" (formerly Second University of Naples), Aversa, Italy, in 2008 and 2005, respectively.

From 2008 to 2017, he worked for many national and international companies as a freelancer. He worked as a software engineer, a senior embedded firmware engineer, a hardware engineer, and a project manager. He was involved in the design of many products for both industrial and consumer electronics; he worked on fleet monitoring systems, thermal printers, electronic scales and cash registers, distributed monitoring systems for photovoltaic plants, Hi-Fi radios and home appliances, automatic end-of-line testing systems, augmented reality devices, and radioactivity measurement instrumentation in collaboration with the National Institute for Nuclear Physics (INFN), Rome, Italy. Since 2018, he has been a Researcher with the University of Campania "Luigi Vanvitelli." His main scientific interests are power measurement theory, design, implementation, and characterization of digital measurement instrumentation and automatic measurement systems, and radioactivity measurements.

Dr. Delle Femine is also a member of the IEEE Instrumentation and Measurement Society.

Carmine Landi (Senior Member, IEEE) was born in Salerno, Italy, in 1955. He received the Laurea degree in electrical engineering from the University of Naples Federico II, Naples, Italy, in 1981.

He was an Assistant Professor of electrical measurement with the University of Naples Federico II from 1982 to 1992. He was an Associate Professor of electrical and electronic measurements with the University of L'Aquila, L'Aquila, Italy, from 1992 to 1999. He has been a Full Professor with the University of Campania "Luigi Vanvitelli" (formerly Second University of Naples), Aversa, Italy, since 1999. He has authored almost 200 international papers in the field of real-time measurement apparatus, automated test equipment, high-precision power measurement, and power quality measurement. His main scientific interests are related to the setup of digital measurement instrumentation, automatic testing of electrical machines, such as asynchronous motors and power transformers, measurement techniques for the characterization of digital communication devices, and the use of digital signal processors for real-time measurements.

Roberto Langella (Senior Member, IEEE) was born in Naples, Italy, in March 1972. He received the Laurea degree in electrical engineering from the University of Naples Federico II, Naples, Italy, in 1996, and the Ph.D. degree in electrical energy conversion from the University of Campania "Luigi Vanvitelli," Aversa, Italy, in 2000.

He is currently a Full Professor of electrical power systems with the University of Campania "Luigi Vanvitelli."

Dr. Langella is also a Senior Member of the IEEE Power Engineering Society. He is also the Chair of the IEEE PES Italy Section and the IEEE PES Task Force on Harmonic Modeling, Simulation and Assessment. He is also an Editor of the IEEE TRANSACTIONS ON POWER DELIVERY.

Mario Luiso (Member, IEEE) was born in Naples, Italy, in July 1981. He received the Laurea degree *(summa cum laude)* in electronic engineering and the Ph.D. degree in electrical energy conversion from the University of Campania "Luigi Vanvitelli" (formerly Second University of Naples), Aversa, Italy, in 2005 and 2007, respectively.

He is currently an Associate Professor with the Department of Engineering, University of Campania "Luigi Vanvitelli." He is the author or a coauthor of more than 150 articles. He has published books, international scientific journals, and conference proceedings. His main scientific interests are related to the development of innovative methods, sensors, and instrumentation for power system measurements, in particular power quality, calibration of instrument transformers, phasor measurement units, and smart meters.

Dr. Luiso is also a member of the IEEE Instrumentation and Measurement Society.

Alfredo Testa (Fellow, IEEE) was born in Naples, Italy, in March 1950. He received the Laurea degree in electrical engineering from the University of Naples Federico II, Naples, in 1975.

He is currently a Professor of Electrical Power Systems with the University of Campania "Luigi Vanvitelli," Aversa, Italy. He is engaged in research on electrical power systems reliability and harmonic analysis.

Dr. Testa is also a fellow of the IEEE Power Engineering Society and the Italian Institute of Electrical Engineers (AEI).